Long-Term Datasets for the Understanding
of Solar and Stellar Magnetic Cycles
Proceedings IAU Symposium No. 340, 2018
D. Banerjee, J. Jiang, K. Kusano & S. Solanki, eds.

doi:10.1017/S1743921318001217

Kinematic and magnetic coherent structures in solar and stellar turbulence

Abraham C.-L. Chian[1,2], Rodrigo A. Miranda[3,4], Erico L. Rempel[2,5] and Brigitte Schmieder[6]

[1]University of Adelaide, School of Mathematical Sciences,
Adelaide SA 5005, Australia.
email: abraham.chian@gmail.com

[2]National Institute for Space Research (INPE),
São José dos Campos SP 12227-010, Brazil.

[3]UnB-Gama Campus, University of Brasília (UnB),
Brasília DF 70910-900, Brazil.

[4]Plasma Physics Laboratory, Institute of Physics, University of Brasília (UnB),
Brasília DF 70910-900, Brazil.

[5]Institute of Aeronautical Technology (ITA),
São José dos Campos SP 12228-900, Brazil.

[6]Observatoire de Paris, LESIA,
5 place Janssen, 92195 Meudon, France.

Abstract. We show that on-off intermittency in solar and stellar cycles is a result of amplitude-phase synchronization in multiscale interactions in solar/stellar dynamos or magnetorotational instability which leads to the formation of kinematic and magnetic coherent structures, and the novel techniques of Lagrangian coherent structures can detect transport barriers and vortices such as magnetic flux tubes/ropes in solar and stellar turbulence with high accuracy.

Keywords. turbulence, Sun: corona, dynamo, photosphere, sunspot cycle

1. Introduction

Long-term behaviour of solar and stellar activities often displays random switching between periods of large- and small-amplitude variations exemplified by grand minima, which can be explained by on-off intermittency driven by solar and stellar turbulence (Rempel *et al.* 2009; Miranda *et al.* 2015). The aim of this paper is to show that: i) on-off intermittency is a result of amplitude-phase synchronization in multiscale interactions in dynamo turbulence which leads to the formation of coherent structures such as magnetic flux tubes/ropes in solar and interplanetary plasmas, responsible for space weather and space climate; ii) the novel techniques of Lagrangian coherent structures (LCS) (Rempel *et al.* 2011; Yeates, Hornig & Welsch 2012; Chian *et al.* 2014; Haller 2015; Rempel *et al.* 2017) can detect transport barriers and vortices such as magnetic flux tubes/ropes in solar interior, photosphere and corona with high precision.

2. On-off intermittency in solar and stellar turbulence

Nonlinear dynamics of long-waves in fluids and drift-waves in plasmas exhibits the behaviour of on-off intermittency at the onset of permanent spatiotemporal chaos, as shown in Figure 1(a) (Chian *et al.* 2010). There is a growing interest to study the role of long-waves such as magnetized Rossby waves in the generation of solar cycles (McIntosh *et al.* 2017). The degree of complexity of on-off states, due to amplitude-phase synchronization

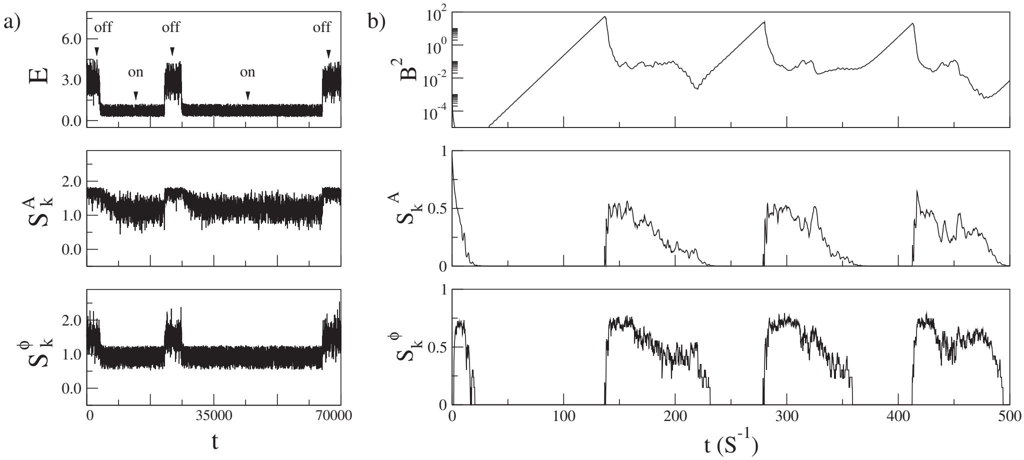

Figure 1. On-off intermittency and amplitude-phase synchronization. Time series of the: (a) wave energy (E), power spectral Shannon entropy (S_k^A), and phase spectral Shannon entropy (S_k^ϕ) for long-wave/drift-wave turbulence; (b) magnetic energy (B^2), power and phase spectral Shannon entropies for magnetorotational instability.

in multiscale interactions, can be quantified by the power and phase spectral Shannon entropies. In the regime of fully-developed turbulence, on-off collective imperfect phase synchronization induces strong bursts of coherent structures in the wave energy in the on-state (He & Chian 2003).

3D MHD simulation of turbulent dynamo forced by an ABC flow displays intermittent features typical of solar and stellar cycles whereby the magnetic field alternates randomly between phases of coherent and incoherent large-scale spatial structures (Rempel *et al.* 2009). The coherent (incoherent) phase is characterized by low (high) values of the power spectral Shannon entropy. 3D MHD simulation of magnetorotational instability in protostellar accretion discs reproduces on-off intermittency studied by Chian *et al.* (2010), as shown in Figure 1(b) (Miranda *et al.* 2015), confirming the key role of amplitude-phase synchronization in multiscale interactions.

3. Kinematic and magnetic coherent structures in solar photosphere and turbulent dynamo

Lagrangian coherent structures in solar photospheric flows in a plage in the vicinity of the active region AR 10930 were investigated by Yeates, Hornig & Welsch (2012) and Chian *et al.* (2010) using the horizontal velocity data derived from Hinode/SOT magnetograms. Yeates, Hornig & Welsch (2012) proposed a direct method to obtain the time-dependent buildup of braided magnetic structures in solar corona by computing the forward finite-time Lyapunov exponent (f-FTLE) and showed that the quasi-separatrix layers represented by the squashing factor (Q_{sq}) (Fig. 2(a)) in coronal magnetic field correspond to repelling Lagrangian coherent structures (rLCS) (Fig. 2(b)) in the photospheric flow. Chian *et al.* (2010) extended this analysis to establish the correspondence of the network of high magnetic flux concentration (Fig. 2(c)) to attracting Lagrangian coherent structures (aLCS) in the photospheric velocity by computing the backward finite-time Lyapunov exponent (b-FTLE) (Fig. 2(d)).

A technique developed by Haller (2015) to detect elliptic LCS based on the Lagrangian averaged vorticity deviation (LAVD) can identify objective kinematic vortices given by

https://doi.org/10.1017/S1743921318001217 Published online by Cambridge University Press

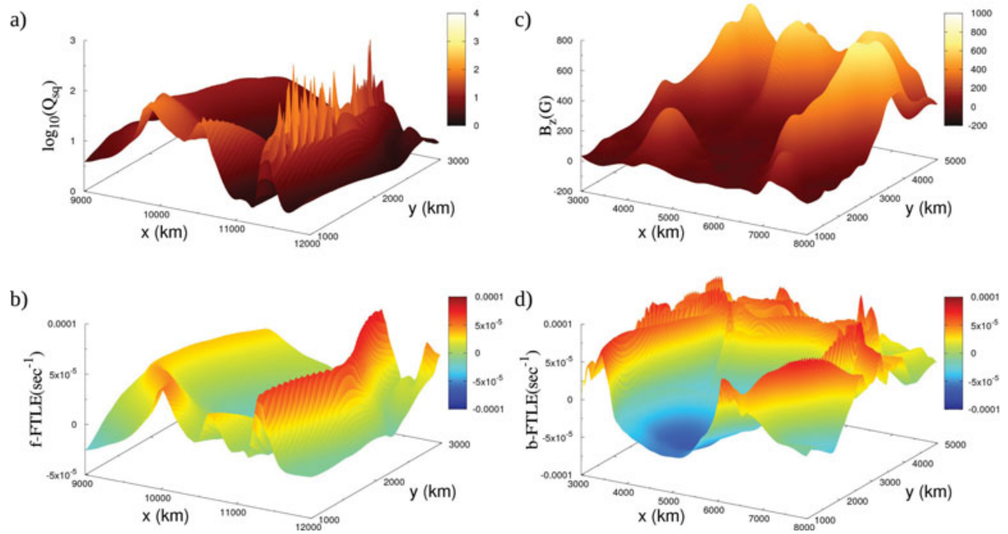

Figure 2. Repelling and attracting Lagrangian coherent structures in the solar photosphere. 3D plots showing the correspondence of (a) the network of quasi-separatrix layers given by the squashing factor (Q_{sq}) at 2006 December 12 14:24 UT, to (b) repelling LCS given by the local maxima of f-FTLE (sec^{-1}) for t_0 = 2006 December 12 14:24 UT and $\tau = +12$ hr; and the correspondence of (c) the network of the magnetic flux concentration given by the line-of-sight magnetic field Bz at t = 2006 December 13 02:24 UT, to (d) attracting LCS given by the local maxima of b-FTLE (sec^{-1}) for t_0 = 2006 December 13 02:24 UT and τ = -12 hr.

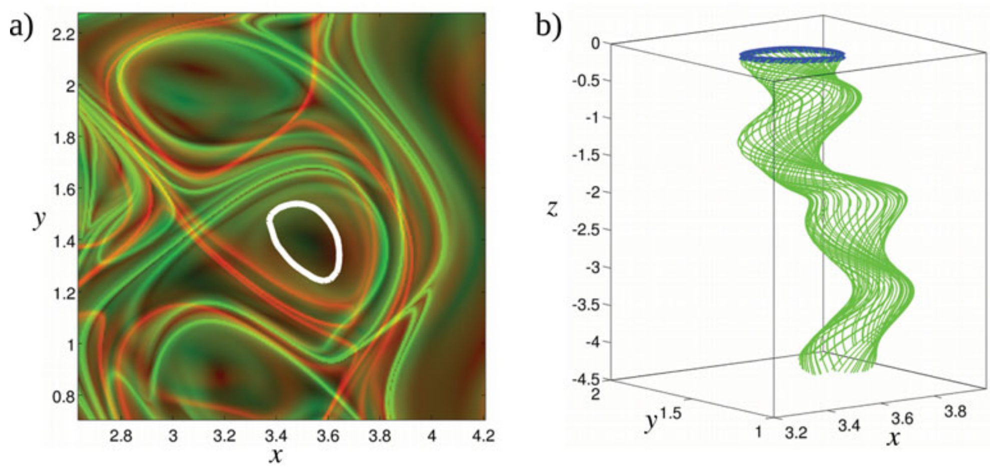

Figure 3. Objective kinematic vortex in turbulent ABC dynamo. (a) 2D view of the boundary (white curve) of an objective kinematic vortex surrounded by the local maxima of forward (green) and backward (red) FTLE fields. (b) 3D view of the objective kinematic vortex showing the pathlines of initial conditions starting from the vortex boundary of Fig. 3a (blue line).

tubular level surfaces of LAVD, which are invariant under time-dependent rotations and translations of the coordinate frame. This technique was adapted by Rempel *et al.* (2017) to detect objective magnetic vortices given by tubular level surfaces of the integrated averaged current deviation. An example of objective kinematic vortex in 3D MHD simulation of turbulent ABC dynamo is shown in Fig. 3(a), where the objective kinematic vortex (white curve) in the x-y plane is surrounded by rLCS and aLCS represented by

https://doi.org/10.1017/S1743921318001217 Published online by Cambridge University Press

lines of the local maxima of f-FTLE (green) and b-FTLE (red) (Rempel *et al.* 2011), respectively. Figure 3(b) shows a 3D view of the objective kinematic vortex given by the pathlines of initial conditions on the vortex boundary (blue line) in Fig. 3(a).

4. Conclusions

Kinematic and magnetic coherent structures such as magnetic flux tubes/ropes are the fundamental intermittent structures of solar and stellar dynamos and turbulence, resulting from amplitude-phase synchronization in multiscale interactions. Lagrangian coherent structures provide an accurate way of identifying transport barriers and kinematic and magnetic vortices in astrophysical turbulence. These novel tools can improve monitoring and prediction of coronal filament eruptions (Zimovets *et al.* 2012; Roudier *et al.* 2018) and understanding of the star-planet relation.

5. Acknowledgments

The authors thank CAPES, CNPq, FAPESP and FAPDF for support.

References

Chian, A. C.-L., Miranda, R. A., Rempel, E. L., Saiki, Y., & Yamada, M. 2010, *Phys, Rev. Lett.*, 104, 254102.

Chian, A. C.-L., Rempel, E. L., Aulanier, A., Schmieder, B., Shadden, S. C., Welsch, B. T., & Yeates, A. R. 2014, *ApJ*, 786, 51.

Haller, G. 2015, *Annu. Rev. Fluid Mech.*, 47, 137.

He, K. & Chian, A. C.-L. 2013, *Phys. Rev. Lett.*, 91, 034102.

McIntosh, S. W., Cramer, W. J., Marcano, M. P., & Leamon, R. J. 2017, *Nature Ast.*, 1, 0086.

Miranda, R. A., Rempel, E. L., & Chian, A. C.-L. 2015, *MNRAS*, 448, 804.

Rempel, E. L., Proctor, M. R. E., & Chian, A. C.-L. 2009, *MNRAS*, 400, 509.

Rempel, E. L., Chian, A. C.-L., & Brandenburg, A. 2011, *ApJL*, 735, L9.

Rempel, E. L., Chian, A. C.-L., Beron-Vera, F. J., Szanyi, S., & Haller, G. 2017, *MNRAS*, 466, L108.

Roudier, T., Schmieder, B., Filippov, B., Chandra, R., & Malherbe, J. M. 2018, *A&A*, submitted.

Zimovets, I., Vilmer, N., Chian, A. C.-L., Sharykin, I., & Struminsky, A. 2012, *A&A*, 547, A6.

Yeates, A. R., Hornig, G., & Welsch, B. T. 2012, *A&A*, 539, A1.